Optics Letters

Polarization-resolved strong light–matter coupling in planar GaAs/AlGaAs waveguides

Pavel Yu. Shapochkin,[1] Maksim S. Lozhkin,[1] Ivan A. Solovev,[1] Olga A. Lozhkina,[1] Yury P. Efimov,[1] Sergey A. Eliseev,[1] Vyacheslav A. Lovcjus,[1] Gleb G. Kozlov,[1] Anastasia A. Pervishko,[2] Dmitry N. Krizhanovskii,[2,3] Paul M. Walker,[3] Ivan A. Shelykh,[2,4] Maurice S. Skolnick,[2,3] and Yury V. Kapitonov[1,*]

[1]Saint-Petersburg State University, ul. Ulyanovskaya 1, St. Petersburg 198504, Russia
[2]ITMO University, St. Petersburg 197101, Russia
[3]Department of Physics and Astronomy, The University of Sheffield, Sheffield, UK
[4]Science Institute, University of Iceland, Dunhagi-3, IS-107, Reykjavik, Iceland
*Corresponding author: kapiton22@gmail.com

Received 12 July 2018; revised 15 August 2018; accepted 16 August 2018; posted 17 August 2018 (Doc. ID 338521); published 14 September 2018

We study the influence of optical selection rules and polarization splittings on properties of exciton polaritons in a planar AlGaAs waveguide containing embedded GaAs quantum wells. We demonstrate that transverse electric and transverse magnetic modes couple differently with light- and heavy-hole quantum well excitons, which leads to distinct polarization splittings of the resulting polariton modes. The experimental data are in good agreement with modeling based on theoretical data for the optical selection rules for quantum well excitons.

https://doi.org/10.1364/OL.43.004526

Polaritons, hybrid light–matter particles arising from strong coupling of light to material excitations such as excitons, represent a unique laboratory for studying a broad variety of quantum and collective phenomena [1]. The very small effective mass of polaritons, inherited from their photonic component, combines with strong interparticle interactions stemming from their excitonic component and favor such phenomena as non- or quasi-equilibrium Bose–Einstein condensation [2–6], Berezinskii–Kosterlitz–Thouless phase transitions [7], superfluid-like behavior [8,9], and formation of vortices [10,11]. The giant $\chi^{(3)}$ effective optical nonlinearity enables generation of amplitude-squeezed light [12] or antibunched polariton emission [13] as well as spontaneous polygon pattern formation [14] and dissipative and conservative bright and dark polariton solitons [15–18]. All these phenomena occur at very low quasiparticle densities.

A number of important properties of polaritons are related to their spin degree of freedom, which is directly related to the polarization of the emitted light. Zero in-plane momentum polaritons with a positive spin projection on the structure growth axis correspond to right circular polarized photons, while polaritons with negative spin projection correspond to left circular polarized photons. For non-zero in-plane momentum, these states become mixed, and the true eigenstates of the non-interacting system are transverse electric (TE) and transverse magnetic (TM) linearly polarized states [19]. Moreover, polariton–polariton interactions are strongly spin dependent, which leads to such effects as polarization multistability and bistability [20,21], vector solitons, and polariton spin switching [22]. There are also theoretical proposals to utilize the polariton polarization degree of freedom in ultrafast optical logic gates operating with polarization domain walls or vector solitons [23].

Up to the present, research has focused nearly exclusively on polaritons in semiconductor microcavities (MCs), which are Fabry–Perot resonators consisting of high-reflectivity Bragg mirrors with quantum wells embedded at an antinode of the cavity mode. Recently, however, alternative systems have been explored. Strong coupling between excitons and Bloch-surface waves [24], Tamm plasmon polaritons [25], and photonic modes in slab waveguides [26] have been demonstrated. In the latter system, polaritons are confined by total internal reflection and propagate with high in-plane momentum and group velocity (30–60 μm/ps), an order of magnitude greater than in MCs. Combined with the ease of patterning, this makes waveguide polariton systems very favorable for the development of ultrafast optical signal processing devices, where light can be controlled by light [27]. In MC systems, the TE–TM photonic splitting is usually small, on the order of 0.1 meV. In the thin single-mode waveguides studied in [26], by contrast, this splitting is on the order of 10's of meV, and so polariton states form predominantly in only the TE or TM polarization. This means that rich physics associated with interaction-induced polarization mixing cannot be addressed in such thin polariton waveguide structures.

In this Letter, we investigate formation of polariton states in slab waveguides with thickness of order 1 μm, where the TE–TM splitting is on the order of 1 meV [28]. Such splitting is comparable to the interaction energy (blue shift) in polariton

condensates and solitons, which paves the way towards the study of spin-dependent phenomena in high-speed interacting polariton fluids and to the development of ultrafast active polariton spin devices. Note that the value of the TE–TM splitting strongly depends on the thickness of a waveguide [29] and can be tuned over a wide range of desired values by varying the thickness of the slab.

The reason for the dependence on thickness is as follows. The resonance condition for a waveguide mode is that the round-trip phase accumulated during propagation, $k_z t$, where t is the thickness, plus the phase ϕ arising from reflection at the two interfaces is an integer multiple of 2π. Here, ϕ is the sum of the phase angles of the Fresnel reflection coefficients at the two interfaces. The TE–TM splitting arises from the difference $\phi_{\mathrm{TE}} - \phi_{\mathrm{TM}}$ and is fixed for a fixed mode index $n_{\mathrm{eff}} = k_x/k_0$, where k_x is the propagation constant (in-plane momentum) of the guided mode, $k_0 = 2\pi/\lambda$, and λ is the free-space wavelength. As t increases, keeping n_{eff} fixed, the importance of the ϕ contribution relative to $k_z t$ becomes less and so the TE–TM splitting reduces.

To demonstrate formation of polariton states in a thick slab waveguide we used a planar asymmetric total internal reflection waveguide with a single quantum well (QW) embedded in the core layer. Sample T699 was grown by molecular beam epitaxy and contains a 930 nm thick $Al_{0.03}Ga_{0.97}As$ core between the vacuum and a 960 nm thick $Al_{0.3}Ga_{0.7}As$ lower cladding. A single 14 nm GaAs QW is located in the center of the core [Fig. 1(a)].

To couple light into the waveguide, a grating coupler was etched on the surface using argon ion beam etching in an Oxford IonFab300 Plus system. The polymethylmethacrylate mask for the grating was prepared using electron-beam lithography in a Zeiss Crossbeam 1540XB microscope equipped with an ELPHY Plus external scan generator. The coupler consisted of a 300 × 300 μm array of grooves with 150 nm width, period 245 nm, and 100 nm depth, as revealed by scanning electron microscopy [Fig. 1(c)]. The sample was cleaved along a GaAs crystallographic plane to create a facet through which light could be collected from the waveguide. The input grating coupler was positioned 80 μm away from the cleaved facet.

The sample was mounted in a closed-cycle helium cryostat and kept at 10 K during the experiments. The grating coupler was illuminated by a tunable diode laser (Sacher Lynx). The laser beam was passed through an intensity stabilizer, Glan prism, and $\lambda/2$ waveplate, allowing control of its intensity and linear polarization, before being focused to a 200 μm spot on the grating coupler using a 150 mm lens. In order to scan the incidence angle φ, a parallel translation of the laser beam across the focusing lens was implemented by refraction in a rotating parallel-sided glass plate. Beam translation before the lens corresponds to varying φ at the focal point. At the QW exciton resonance wavelength and for the chosen grating period, light close to normal incidence is coupled to the guided mode by first-order diffraction.

Coupled light propagated through the waveguide and was collected from the sample edge before being refocused onto a photomultiplier. Fast scanning of the incident angle φ in the range of $-20\ldots+20°$ combined with slow scanning of the laser photon energy E from 1.49 to 1.57 eV made it possible to measure the dispersion (dependence of the waveguide transmission spectrum on the incidence angle) for all three waveguide modes and both heavy hole (HH) and light hole (LH) exciton resonances in the QW.

Reflection spectroscopy of sample at 8 K revealed pronounced HH (HH-exc) ($E_{\mathrm{HH}} = 1.526$ eV) and LH-exc ($E_{\mathrm{LH}} = 1.530$ eV) exciton resonances [Fig. 2(b)]. Besides the excitonic resonances, waveguide transmission measurements at energies below the excitons revealed maxima corresponding to the three electromagnetic modes. The waveguide is expected to support two even (#0 and #2) modes and one odd (#1) mode having an antinode and a node at the position of the QW layer, respectively [Fig. 1(b)]. All the photon modes

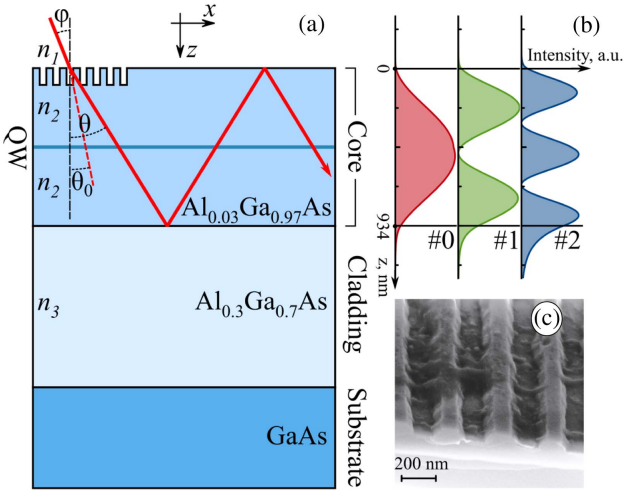

Fig. 1. (a) Experimental geometry. The guided mode is excited using the diffraction grating coupler, and is collected from the sample edge. (b) Electric field distribution of three TE-polarized modes (#0, #1, and #2) in the waveguide. (c) Electron microscope image of a section of the grating coupler reveals the 150 nm width and 100 nm depth of the stripes.

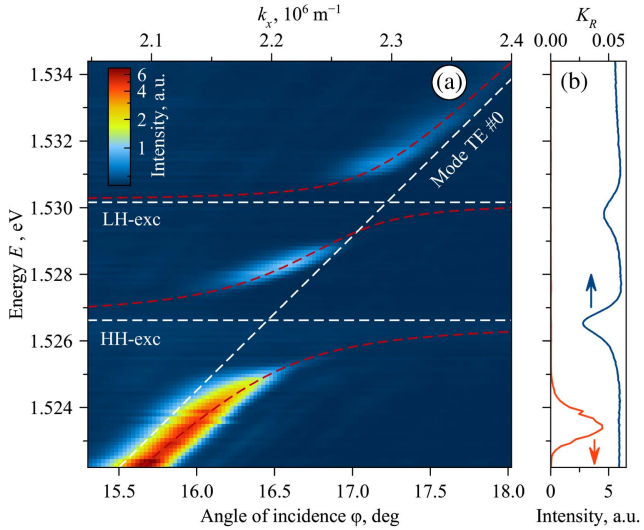

Fig. 2. (a) Waveguide transmission spectra as a function of incident angle φ or x component of the wave vector k_x for mode #0 and TE polarization. Intensity is shown on a logarithmic color scale. Photon and exciton modes (white dashed), best fit to a coupled oscillator model (red dashed). (b) Reflection spectra in TM polarization and $\varphi = 74°$ (blue), and transmission spectra in TE polarization at $\varphi = 16°$ (red).

have nearly the same group velocity $\frac{\partial E}{\partial k_x}$, but they have different TE–TM polarization splittings. Mode #0 has the smallest TE–TM splitting of 0.6 meV. The TE–TM splitting increases to 2.2 meV and 4 meV for the higher order modes #1 and #2, respectively.

TE–TM splitting increases as the mode number increases. For modes far above cutoff, the light propagates at an angle $\theta \approx 90°$ (e.g., parallel to the interfaces; see Fig. 1) and $\cos\theta \approx 0$, so that the Fresnel coefficients for TE and TM modes are approximately equal, and there is very little splitting. Higher-order modes propagate at steeper angles θ leading to an increasing difference in ϕ_{TE} and ϕ_{TM} and increasing splitting. This occurs as long as n_{eff} is much larger than the index of at least one of the cladding materials, which is always the case here because of the large index contrast between GaAs and air.

The spectral (angular) full width at half-maximum (FWHM) of the modes was around 1 meV (0.2°), so that the quality factor is better than $Q = \frac{\Delta\lambda}{\lambda} \approx 1800$ [Fig. 2(b)]. The measured linewidth is mostly determined by the photon loss rate due to coupling to the free-space modes in the grating region. The high measured Q-factor is supported by the observation of light propagation in the waveguide at millimeter distances for wavelengths away from the exciton resonances.

Figure 2 shows the waveguide transmission spectrum as a function of incidence angle on the grating for TE-polarized light, for photon energies near the exciton resonances, and wavenumbers in the vicinity of mode #0. The spectrum reveals an anticrossing of the photon mode with both the LH-exc and HH-exc characteristics of the expected behavior for strong light–matter coupling. Three polariton branches are formed. Light–matter coupling is accompanied by the attenuation of the transmitted intensity for energies close to the exciton resonances. Simultaneously, the FWHM of the polariton branches reduces to 0.2 meV, indicating low inhomogeneous broadening of the exciton resonances. The spectral peaks were fitted by Gaussian functions, and the angle-energy dependence (polariton dispersions) are depicted for the different modes and two polarizations in Fig. 3.

To provide a fit to the experimentally measured polariton dispersions, we use a model of three coupled oscillators, one corresponding to the photon mode and two others to the HH and LH-excitons, respectively (see the red dashed curves in Fig. 2). The corresponding secular equation reduces to the following third-order algebraic equation:

$$E_{\mathrm{ph}}(\varphi) - E_{\mathrm{pol}}(\varphi) = \frac{\Omega_{\mathrm{HH}}^2}{4(E_{\mathrm{HH}} - E_{\mathrm{pol}}(\varphi))} + \frac{\Omega_{\mathrm{LH}}^2}{4(E_{\mathrm{LH}} - E_{\mathrm{pol}}(\varphi))}, \tag{1}$$

where Ω_{HH} and Ω_{LH} are, respectively, the Rabi-splittings for HH-exc and LH-exc, φ is the angle of incidence on the grating coupler, $E_{ph}(\varphi)$ is the dispersion of the photon mode, and $E_{pol}(\varphi)$ is the polariton dispersion. The Rabi splittings extracted from the fits to the the experimental data are shown in Table 1.

For the odd mode, #1, no strong coupling is observed for either exciton resonance in either polarization. This is as expected, since the QW is located at a node of the electromagnetic field. Nevertheless a slight attenuation and hint of a small splitting (around 1 meV) could be seen around the LH-exc in the TM polarization. This may be due to the slight shift in the field node from the center of the core layer due to the asymmetry introduced by the different cladding refractive indices on either side of the structure.

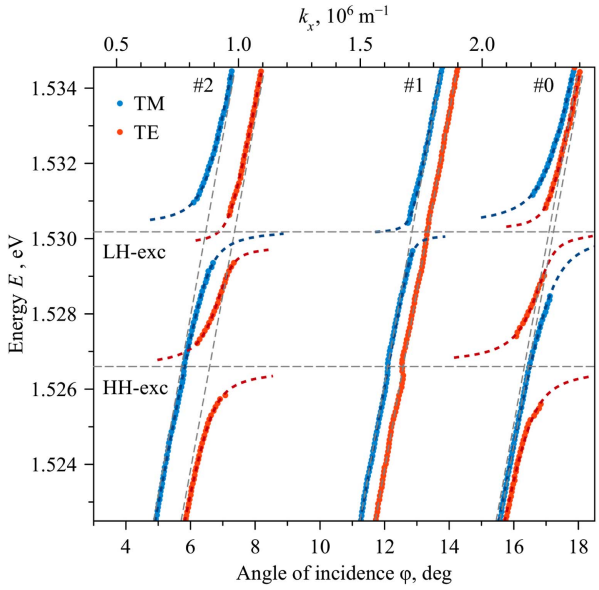

Fig. 3. Dispersion of the modes of a planar waveguide with a single quantum well placed in the middle of a core layer. Experimental data are shown by colored markers, and dashed lines represent fit by the anticrossing model. Note the absence of strong coupling between TM modes and HH-exc.

Table 1. Experimentally Determined Rabi Splittings Ω, meV for Even Photonic Modes and HH-exc and LH-exc Transitions

	Mode #0		Mode #2	
Polarization	**HH**	**LH**	**HH**	**LH**
TE (in-plane)	3.1	1.8	2.5	1.6
TM (nearly normal)	0	3.6	0	2.8

Our experimental data are in agreement with well-known polarization-dependent selection rules for HH and LH-exciton transitions in GaAs/AlGaAs QWs [30], as seen in Table 2. We see that switching from TE to TM polarization leads to the disappearance of the strong coupling for the HH-exc resonance, whereas the coupling to the LH-exc reaches its maximum (see Fig. 3), which is fully in accord with the expected qualitative trend, where the HH transition is forbidden for TM polarization (see Table 2). Quantitatively, the ratios between the observed values of Rabi splittings Ω correspond well to those predicted by the oscillator strengths f of the transitions. Our experimental oscillator strength ratios are compared to those expected theoretically in Table 2, where we use $\Omega \propto \sqrt{f}$ (following [31]). The values of the Rabi splittings for different modes and polarizations vary from 1.6 meV to 3.6 meV. This is smaller than the 5–6 meV observed in [26] for TE-polarized polaritons in a 135 nm thick AlGaAs/GaAs waveguide with a 10 nm $In_{0.04}Ga_{0.96}As$/GaAs single QW as the active region. The difference is due to the greater thickness of the waveguide used in the present work, which reduces the spatial overlap of photon and exciton fields in the growth direction.

Table 2. Optical Selection Rules for QW Excitons Represented as Oscillator Strength of the Corresponding Transition Divided by the Oscillator Strength of HH Transition in TE Polarization

Polarization	HH-exc	LH-exc
TE, theory	1	$\frac{1}{3}$
TE, mode #0	1	0.34
TE, mode #2	1	0.4
TM, theory	0 (forbidden)	$\frac{4}{3}$
TM, mode #0	0	1.34
TM, mode #2	0	1.25

Theoretical values are taken from [30]; experimental values are extracted from Table 1 with use of the formula $\Omega \sim \sqrt{f}$ by division of squared values of corresponding Rabi splittings.

In conclusion, we have studied polarization-resolved polariton dispersions in a thick planar AlGaAs total internal reflection waveguide with a thin GaAs QW embedded inside the core layer. We have demonstrated the strong influence of the polarization-dependent optical selection rules and the TE–TM splitting of the waveguide modes on the properties of propagating polaritons. Despite the reduced Rabi splitting, the very narrow HH and LH exciton linewidths in the GaAs QW of this work lead to well-resolved narrow polariton modes. This property, as well as the small values of TE–TM splitting (TE–TM splitting for LH exciton polaritons decreases with increasing exciton fraction), may enable the study of interesting spin-dependent quantum fluid phenomena and applications (vector dark and bright solitons, polarization-dependent switching, etc.) in such high-speed waveguide polariton systems.

Funding. Ministry of Education and Science of the Russian Federation (Minobrnauka) (Megagrant 14.Y26.31.0015, Goszadanie no. 3.2614.2017/4.6); Icelandic Centre for Research (RANNIS) (163082-051); Russian Science Foundation (RSF) (18-72-00058).

Acknowledgment. I. A. Sh. acknowledges support from the Ministry of Education and Science of Russian Federation and Icelandic Research Fund. A. A. P. acknowledges the support from RSF. The experiment was carried out using equipment of the SPbU Resource Center "Nanophotonics." We thank S. V. Poltavtsev, I. V. Iorsh, and L. L. Litvin (Raith GmbH) for fruitful discussions.

REFERENCES

1. A. V. Kavokin, J. J. Baumberg, G. Malpuech, and F. P. Laussy, *Microcavities* (Oxford University, 2017).
2. J. Kasprzak, M. Richard, S. Kundermann, A. Baas, P. Jeambrun, J. M. J. Keeling, F. M. Marchetti, M. H. Szymanska, R. Andre, J. L. Staehli, V. Savona, P. B. Littlewood, B. Deveaud, and L. S. Dang, Nature **443**, 409 (2006).
3. R. Balili, V. Hartwell, D. Snoke, L. Pfeiffer, and K. West, Science **316**, 1007 (2007).
4. A. P. D. Love, D. N. Krizhanovskii, D. M. Whittaker, R. Bouchekioua, D. Sanvitto, S. Al Rizeiqi, R. Bradley, M. S. Skolnick, P. R. Eastham, R. André, and L. S. Dang, Phys. Rev. Lett. **101**, 067404 (2008).
5. D. N. Krizhanovskii, K. G. Lagoudakis, M. Wouters, B. Pietka, R. A. Bradley, K. Guda, D. M. Whittaker, M. S. Skolnick, B. Deveaud-Plédran, M. Richard, R. André, and L. S. Dang, Phys. Rev. B **80**, 045317 (2009).
6. Y. Sun, P. Wen, Y. Yoon, G. Liu, M. Steger, L. N. Pfeiffer, K. West, D. W. Snoke, and K. A. Nelson, Phys. Rev. Lett. **118**, 016602 (2017).
7. D. Caputo, D. Ballarini, G. Dagvadorj, C. S. Muñoz, M. De Giorgi, L. Dominici, K. West, L. N. Pfeiffer, G. Gigli, F. P. Laussy, M. H. Szymańska, and D. Sanvitto, Nat. Mater. **17**, 145 (2018).
8. A. Amo, D. Sanvitto, F. P. Laussy, D. Ballarini, E. del Valle, M. D. Martin, A. Lemaître, J. Bloch, D. N. Krizhanovskii, M. S. Skolnick, C. Tejedor, and L. Viña, Nature **457**, 291 (2009).
9. A. Amo, J. Lefrére, S. Pigeon, C. Adrados, C. Ciuti, I. Carusotto, R. Houdré, E. Giacobino, and A. Bramati, Nat. Phys. **5**, 805 (2009).
10. K. G. Lagoudakis, M. Wouters, M. Richard, A. Baas, I. Carusotto, R. André, L. S. Dang, and B. Deveaud-Plédran, Nat. Phys. **4**, 706 (2008).
11. D. Sanvitto, F. M. Marchetti, M. H. Szymańska, G. Tosi, M. Baudisch, F. P. Laussy, D. N. Krizhanovskii, M. S. Skolnick, L. Marrucci, A. Lemaître, J. Bloch, C. Tejedor, and L. Viña, Nat. Phys. **6**, 527 (2010).
12. T. Boulier, M. Bamba, A. Amo, C. Adrados, A. Lemaitre, E. Galopin, I. Sagnes, J. Bloch, C. Ciuti, E. Giacobino, and A. Bramati, Nat. Commun. **5**, 3260 (2014).
13. G. Muñoz-Matutano, A. Wood, M. Johnson, X. V. Asensio, B. Baragiola, A. Reinhard, A. Lemaitre, J. Bloch, A. Amo, B. Besga, M. Richard, and T. Volz, arXiv:1712.05551 (2018).
14. C. E. Whittaker, B. Dzurnak, O. A. Egorov, G. Buonaiuto, P. M. Walker, E. Cancellieri, D. M. Whittaker, E. Clarke, S. S. Gavrilov, M. S. Skolnick, and D. N. Krizhanovskii, Phys. Rev. X **7**, 031033 (2017).
15. M. Sich, D. N. Krizhanovskii, M. S. Skolnick, A. V. Gorbach, R. Hartley, D. V. Skryabin, E. A. Cerda-Méndez, K. Biermann, R. Hey, and P. V. Santos, Nat. Photonics **6**, 50 (2012).
16. V. Goblot, H. S. Nguyen, I. Carusotto, E. Galopin, A. Lemaître, I. Sagnes, A. Amo, and J. Bloch, Phys. Rev. Lett. **117**, 217401 (2016).
17. P. M. Walker, L. Tinkler, B. Royall, D. V. Skryabin, I. Farrer, D. A. Ritchie, M. S. Skolnick, and D. N. Krizhanovskii, Phys. Rev. Lett. **119**, 097403 (2017).
18. D. V. Skryabin, Y. V. Kartashov, O. A. Egorov, M. Sich, J. K. Chana, L. E. Tapia Rodriguez, P. M. Walker, E. Clarke, B. Royall, M. S. Skolnick, and D. N. Krizhanovskii, Nat. Commun. **8**, 1554 (2017).
19. I. A. Shelykh, A. V. Kavokin, Y. G. Rubo, T. C. H. Liew, and G. Malpuech, Semicond. Sci. Technol. **25**, 013001 (2010).
20. N. A. Gippius, I. A. Shelykh, D. D. Solnyshkov, S. S. Gavrilov, Y. G. Rubo, A. V. Kavokin, S. G. Tikhodeev, and G. Malpuech, Phys. Rev. Lett. **98**, 236401 (2007).
21. T. K. Paraïso, M. Wouters, Y. Léger, F. Morier-Genoud, and B. Deveaud-Plédran, Nat. Mater. **9**, 655 (2010).
22. A. Amo, T. H. C. Liew, C. Adrados, R. Houdre, E. Giacobino, A. V. Kavokin, and A. Bramati, Nat. Photonics **4**, 361 (2010).
23. T. C. H. Liew, I. A. Shelykh, and G. Malpuech, Physica E **43**, 1543 (2011).
24. G. Lerario, D. Ballarini, A. Fieramosca, A. Cannavale, A. Genco, F. Mangione, S. Gambino, L. Dominici, M. D. Giorgi, G. Gigli, and D. Sanvitto, Light Sci. Appl. **6**, e16212 (2017).
25. M. Wurdack, N. Lundt, M. Klaas, V. Baumann, A. V. Kavokin, S. Höfling, and C. Schneider, Nat. Commun. **8**, 259 (2017).
26. P. M. Walker, L. Tinkler, M. Durska, D. M. Whittaker, I. J. Luxmoore, B. Royall, D. N. Krizhanovskii, M. S. Skolnick, I. Farrer, and D. A. Ritchie, Appl. Phys. Lett. **102**, 012109 (2013).
27. F. Marsault, H. S. Nguyen, D. Tanese, A. Lemaître, E. Galopin, I. Sagnes, A. Amo, and J. Bloch, Appl. Phys. Lett. **107**, 201115 (2015).
28. P. Y. Shapochkin, Y. V. Kapitonov, S. V. Poltavtsev, M. S. Lozhkin, O. A. Lozhkina, A. D. Manukhovaa, Y. P. Efimov, S. A. Eliseev, V. A. Lovtsyus, V. V. Petrov, I. A. Solovev, and G. G. Kozlov, Opt. Spectrosc. **122**, 303 (2017).
29. A. W. Snyder and J. Love, *Optical Waveguide Theory* (Chapman & Hall, 1983).
30. G. Bastard, *Wave Mechanics Applied to Semiconductor Heterostructures* (Les Éditions de Physique, Halsted, 1988).
31. V. Savona, L. C. Andreani, P. Schwendimann, and A. Quattropani, Solid State Commun. **93**, 733 (1995).